A Zinc(II)/Lead(II)/Cadmium(II)-Inducible Operon from the Cyanobacterium *Anabaena* Is Regulated by AztR, an α3N ArsR/SmtB Metalloregulator†

Tong Liu,‡ James W. Golden,§ and David P. Giedroc*,‡

Department of Biochemistry and Biophysics, 2128 TAMU, Texas A&M University, College Station, Texas 77843-2128, and Department of Biology, 3258 TAMU, Texas A&M University, College Station, Texas 77843-3258

Received March 10, 2005; Revised Manuscript Received April 22, 2005

ABSTRACT: A novel Zn(II)/Pb(II)/Cd(II)-responsive operon that consists of genes encoding a Zn(II)/Pb(II) CPx-ATPase efflux pump (*aztA*) and a Zn(II)/Cd(II)/Pb(II)-specific SmtB/ArsR family repressor (*aztR*) has been identified and characterized from the cyanobacterium *Anabaena* PCC 7120. In vivo real time quantitative RT-PCR assays reveal that both *aztR* and *aztA* expression are induced by divalent metal ions Zn(II), Cd(II), and Pb(II) but not by other divalent [Co(II), Ni(II)] or monovalent metal ions [Cu(I) and Ag(I)]. The introduction of a plasmid containing the *azt* operon into a Zn(II)/Cd(II)-hypersensitive *Escherichia* coli strain GG48 functionally restores Zn(II) and Pb(II) resistance with a limited effect on Cd(II) resistance. Gel mobility shift assays and *azt*R O/P-lacZ induction experiments confirm that AztR is the metal-regulated repressor of this operon. In vitro biochemical and mutagenesis studies indicate that AztR contains a sole metal-binding site, designated the α3N site, that binds Zn(II), Cd(II), and Pb(II) with a high affinity. Optical absorption spectra of Co(II)- and Cd(II)-substituted AztR and ^{113}Cd NMR spectroscopy of ^{113}Cd(II)-substituted AztR reveal that the sole α3N site in AztR is a CadC-like distorted tetrahedral S_3(N,O) metal site. The first metal-coordination shell in the AztR α3N site differs from other α3N family members that sense Cd(II)/Pb(II) and those α5 repressors that sense Zn(II)/Co(II). Our results reveal that the α3N site in AztR mediates derepression of the *azt* operon in the presence of Zn(II), as well as Cd(II) and Pb(II); this might have provided *Anabaena* with an evolutionary advantage to adapt to heavy-metal-rich environments, while maintaining homeostasis of an essential metal ion, Zn(II).

Zinc is one of the most important biologically essential trace elements in all kingdoms of life. Zinc functions as a cofactor in over 300 enzymes spanning all six classes of enzymes that function in a wide variety of metabolic processes (*1*−*3*). Genetic and structural studies over the past decade have provided considerable insight into zinc homeostasis in living cells. Just like other essential metal ions, zinc homeostasis in cells is governed by two important processes. Under conditions of limiting metal ion concentrations, the uptake of essential metal ions from the environment and transfer to cellular compartments for optimal metalloprotein activity is induced, with the intracellular metal ion concentration maintained at an appropriate level through detoxification, efflux, or sequestration of excess metal under metal-replete conditions.

In *Escherichia coli*, Zn(II) homeostasis is under the control of two metal-sensitive transcriptional regulators. These are Zur, a Fur-family homologue, and ZntR, a Mer-family activator, which control the transcription of genes encoding the metallotransporters ZnuABC[1] and ZntA, respectively, in a zinc-regulated fashion (*1*, *4*, 5). Similar zinc homeostasis systems have been proposed to operate in a wide range of microbial systems. ZntA, a member of the Zn(II)/Cd(II)/Pb(II)-transporting CPx-ATPase subgroup, belongs to a subfamily of a large family of cation-transport membrane proteins (CPx-ATPases) (*6*). Another subgroup of this superfamily is Cu(I)/Ag(I)-transporting ATPases, which have been found in both eukaryotes and bacteria (*7*, 8). The CPx-type ATPases are characterized by a -CPx- sequence found in the sixth transmembrane helix which is thought to function as the major allosteric effector of ATPase activity and a metal specificity determinant of each subfamily of ATPases (*9*). The mechanism of metal recognition and metal specificity in CPx-ATPases is still largely unknown. However, it is known that Cu(I)/Ag(I)-responsive CPx-ATPases usually have one to six "CxxC" metal-binding domains (MBDs) in their cytosolic N-terminal domains, whereas all characterized Zn(II)/Cd(II)/Pb(II)-transporting CPx-ATPases, such as *E. coli* ZntA or *Oscillatoria brevis* Bxa1, possess just one MBD domain or His-rich putative metal-binding domain (*10*−*13*).

Inspection of the full genomic sequence of the cyanobacterium *Anabaena* PCC 7120 reveals a putative zinc homeostasis system similar to that of *E. coli* (Figure 1). Like *E.*

† This work was supported by grants from the National Institutes of Health (GM042569) and the Robert A. Welch Foundation (A-1295) to D.P.G.

* To whom correspondence should be addressed. E-mail: giedroc@tamu.edu. Tel: 979-845-4231. Fax: 979-845-4946.

‡ Department of Biochemistry and Biophysics, Texas A&M University.

§ Department of Biology, Texas A&M University.

[1] Abbreviations: ABC, ATP-binding cassette; *azt*, *Anabaena* zinc transport; *azu*, *Anabaena* zinc uptake; mag-fura-2, 2-[6-[bis(carboxymethyl)amino]-5-(carboxymethoxy)-2-benzofuranyl]-5-oxazolecarboxylic acid; MBD, metal-binding domain (based on the fold of the yeast copper chaperone Atx1); O/P, operator/promoter; ONPG, *o*-nitrophenyl *β*-D-galactopyranoside.

10.1021/bi050450+ CCC: $30.25
Published on Web 05/27/2005

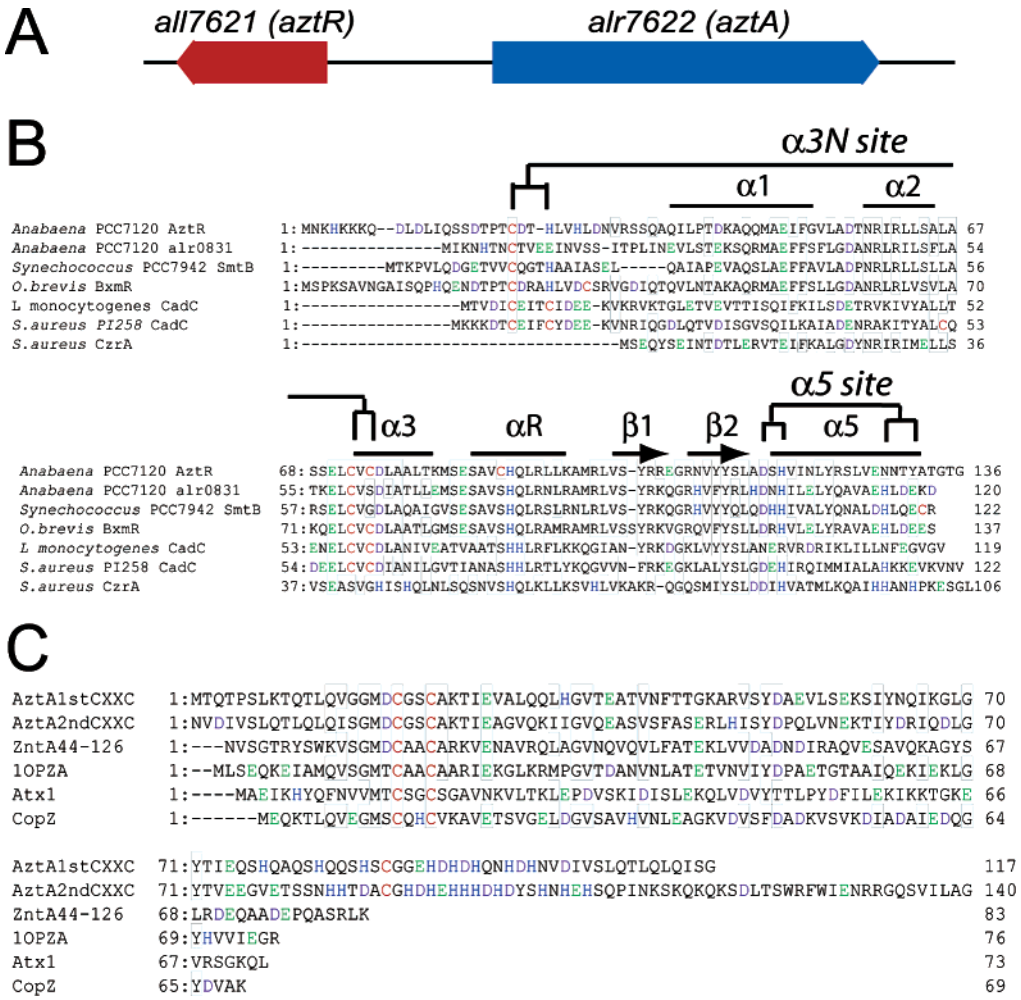

FIGURE 1: The chromosomally encoded Zn(II)/Pb(II)/Cd(II)-responsive *azt* operon AztA/R in *Anabaena* PCC 7120. (A) Schematic representation of the operon. (B) Sequence alignment of AztR with other ArsR/SmtB family metalloregulatory transcriptional repressors. The proposed metal-binding ligands in the α3N site and the α5 site are denoted above the secondary structure assignment derived from crystallographic studies of CzrA and SmtB (*16*). (C) Sequence alignment of two metal-binding domain (MBD)/His-rich domains in the N-terminal region of AztA with analogous domains associated with two CPx-ATPases and two Cu(I) chaperones. The sequences above are the first and second N-terminal repeats of AztA in *Anabaena* PCC 7120, Zn(II) transporting CPx-ATPase (ZntA) from *E. coli*, *Bacillus subtilis* Cu(I) transporting CPx-ATPase CopA (10PZA), *Saccharomyces cerevisiae* Cu(I) chaperone Atx1, and *B. subtilis* Cu(I) chaperone CopZ. Potential metal-binding residues Glu (colored green), Asp (purple), His (blue), and Cys (red) are color-coded according to residue type in panels B and C.

coli, this system appears to consist of a single CPx-ATPase (alr7622, denoted *aztA*[1] here) and a putative ZnuABC homologue ABC transporter (all0833, all0832, and all0831, termed AzuABC[1] here). In striking contrast to *E. coli*, there are no ZntR or Zur homologues in close proximity to those genes. Instead, two ArsR/SmtB family repressors are found just upstream of the gene encoding AztA[1] (all7621) and between open reading frames (ORFs), all0830 and all0832 (alr0831), respectively.

The ArsR/SmtB family of transcriptional repressors are homodimeric, winged helix DNA binding proteins that repress the expression of their respective operon and induce derepression by binding specific metal ions. ArsR/SmtB proteins usually harbor one or both of two structurally distinct metal-binding sites, designated α3N and α5, each of which contain three or four conserved metal ligands (Figure 1) (*14*). The α5 site-mediated mechanism of regulation of operator/promoter binding by Zn(II) in zinc sensors *Staphylococcus aureus* CzrA and *Synechoccocus* SmtB is well understood structurally and depends critically on a key metal-liganding histidine that corresponds to His[97] in CzrA and His[117] in SmtB (*16*). In contrast to zinc sensors CzrA and SmtB, CadCs encoded by *S. aureus* plasmid pI258 and *Listeria monocytogenes* utilize a distinct thiolate-rich metal-sensing site termed α3N to metalloregulate the expression of a Cd(II)/Pb(II) efflux pump, CadA (*17*) (Figure 1). How metal ions drive α3N site-mediated negative regulation of DNA binding remains unknown.

As a first step in the characterization of the zinc homeostasis system in *Anabaena* PCC 7120, we show here that the *aztAR* operon is Zn(II)/Pb(II)/Cd(II)-inducible and that AztR is a Zn(II)/Pb(II)/Cd(II)-responsive metalloregulator. AztR utilizes the α3N metal-binding site to sense both essential Zn(II) and toxic Pb(II)/Cd(II) ions. The cobalt and cadmium optical spectra and the ^{113}Cd NMR spectrum suggest that the α3N metal-binding site in AztR is a tetrahedral S_3(N,O) metal site that is distinct from other CadC-like Cd(II)/Pb(II) α3N and α5 sensor N_3O sites specific for Zn(II)/Co(II). AztA is a Zn(II)-translocating CPx-ATPase, which is induced by Zn(II)/Cd(II)/Pb(II) and confers significant resistance to Zn(II) and Pb(II) salts but limited tolerance to Cd(II) salts in vivo. Our results suggest that the

particular structural characteristics of the AztR α3N site, relative to previously characterized α3N and α5 sites, are ideally suited to effect metalloregulation by Zn(II) as well as the larger more thiophilic metal ions Cd(II) and Pb(II). This characteristic may have endowed *Anabaena* with an evolutionary advantage by allowing it to adapt to heavy-metal-rich environments.

MATERIALS AND METHODS

Cell Culture and DNA Manipulations. Anabaena PCC 7120 was grown in BG-11 medium at 30 °C with continuous illumination from fluorescent lamps as described (*20*). LB or minimal media was used to cultivate *E. coli* strains XL-1 blue, BL21(DE3), and GG48 (ΔzitB::Cm *zntA*::Km) (*21*). For metal tolerance experiments, the *aztR* gene, the *aztA* gene, or the entire *aztAR* operon was amplified from genomic DNA of *Anabaena* PCC 7120. The resulting PCR fragments were cloned into the pET3a (Novagen) using *Nde*I and *Eco*RI sites to create pETAztR and pETAztA. *Bgl*II and *Eco*RI sites were used for construction of the pETAztR/A plasmid which includes the entire *aztAR* operon. A PCR-based quick-change method was employed for substitution of Cys74 to Ser using pETAztR as a template (designated pETAztR_C74S). For the AztR-LacZ fusion construct, a 593 bp sequence upstream of AztA, which includes *aztR* and the entire *aztA/R* operator-promoter region, was amplified by PCR and fused to a promoterless *lacZ* gene in pBlue-TOPO vector (Invitrogen), with the resulting plasmid (TOPO-aztO/P) transformed into TOP10 cells after being confirmed by DNA sequencing. Genomic DNA and total RNA were isolated from *Anabaena* strain PCC 7120 as described previously (*22*). Metal salt solutions were prepared by the addition of 1.0 M Zn(II), Cd(II), Pb(II), Co(II), Ni(II), Cu(II), and Ag(I) stock solutions, with the concentrations determined by atomic absorption spectroscopy. Note that although Cu salts were added to growth media as copper(II) sulfate, the form of the metal inside cells is likely to be Cu(I) as indicated.

Real Time Quantitative RT-PCR (rQRT-PCR). Anabaena strain PCC 7120 was grown in BG-11 medium at 30 °C for about 7 days until the optical density reached ≈0.5 (OD_{750}), after which time metal salts [$ZnSO_4$, $CdCl_2$, $Pb(OAc)_2$, $CoCl_2$, $NiCl_2$, $CuCl_2$, and $AgNO_3$] were added into growing cultures at the indicated concentrations. After incubation for 2 h, cells were collected by centrifugation and then used for RNA isolation. The absolute amount of *aztR* or *aztA* mRNAs induced by metal ions was quantified by rQRT-PCR using an external standard as described before (*23*). Quantitative RT-PCR was performed with Gene amp 7900HT, using the One step Real time RT-PCR kit (Qiagen). Total RNA (10 ng) was used in each reaction. RNase P subunit B (*rnpB*) mRNA was employed as a positive control in all samples. The integrity of amplification of target fragments was confirmed by melting curve analysis of PCR products and DNA sequencing.

β-Galactosidase Assays. E. coli GG48 cell cultures transformed with TOPO-aztO/P were grown at 30 °C overnight in 10 mL of minimal medium supplemented with 50 μg/mL ampicillin. Five microliters of each overnight culture was inoculated into 10 mL of fresh minimal medium. After incubation for 3 h ($OD_{600} \approx 0.4$), the indicated total concentration of metal ion was added to the cultures, and the cells were harvested 5 h later. β-Galactosidase activity was determined with *o*-nitrophenyl β-D-galactopyranoside (ONPG) as the substrate using a β-galactosidase assay kit (Invitrogen).

Metal Sensitivity Assays. The pETAzt and pET3a plasmids were transformed into *E. coli* strain GG48 with the transformants cultivated overnight at 37 °C in LB medium supplemented with 100 μg/mL ampicillin. Cultures were then diluted 1:50 into 10 mL of fresh LB media supplemented with the indicated concentration of heavy metal salts. The optical density of the resulting cultures was determined at 600 nm after incubation for 8 h.

Protein Purification. Wild-type and C74S AztR were expressed in *E. coli* BL21 transformed with pETAztR and pETAztR_C74S. After 4 h of induction, the cells were harvested, and AztRs were purified using a modified procedure based on that described before for SmtB (*24*). Following cation-exchange HPLC, size-exclusion chromatography, and anion-exchange HPLC on an Akta-10 purifier, the purified AztRs were dialyzed against 3 L of buffer S (10 mM HEPES, 0.4 M NaCl, pH 7.0) in an anaerobic Vacuum Atmospheres glovebox. Final protein purity was determined to be ≥95% by Coomassie-stained 18% Tricine−SDS−PAGE gels. The concentration of AztR was determined using absorbance at 280 nm, with molar extinction coefficients of $\epsilon_{AztR} = 7950\ M^{-1}\cdot cm^{-1}$ and $\epsilon_{AztRC74S} = 7825\ M^{-1}\cdot cm^{-1}$ at 280 nm determined by amino acid analysis carried out by the Texas A&M University Protein Chemistry Laboratory. The number of free thiols in AztRs was determined by using an anaerobic DTNB colorimetric assay as described (*24*). Typical preparations of wild-type AztR have 3.8 free thiols (4 expected), with 2.7 (3 expected) obtained for the C74S AztR.

Electrophoretic Mobility Shift Assays (EMSAs). A 200 bp region between AztR and AztA ORFs was divided into five overlapping DNA fragments of 80 bp to create EMSA probes F1−F5 (see Figure 3), with about 50 bp overlapping on either end. The 3′-end of each DNA fragment was labeled with digoxigenin (DiG) using the DiG-Gel shift kit (Roche Applied Science) with the EMSA assay carried out as described previously (*22*). The DiG-labeled DNA and AztR monomer concentrations used in this experiment were 1.0 nM and 0.67 μM, respectively.

In Vitro Metal-Binding Experiments. Metal ion-binding experiments for Co(II), Cd(II), and Pb(II) were carried out anaerobically at 25 °C in a Hewlett-Packard model 8452A exactly as described previously (*18*, *24*). For Co(II) titrations, a monomer concentration range of 95−120 μM was used; for the Cd(II) and Pb(II) titrations, 40−60 μM protein was used. Buffer H (10 mM Bis-Tris, 0.4 M NaCl, pH 7.0) was employed for Pb(II) titrations, and buffer S was used for other metal ions. The absorption spectrum for each trial was measured before and following each aliquot of metal ion solution. The titration curves were generated by subtraction of the initial spectrum (apoprotein) from subsequent ones and corrected for dilution and background subtraction as described previously. All binding curves were fit with a two-step metal-binding model assuming a nondissociable AztR homodimer, with K_{M1} and K_{M2} resolved from these fits. Anaerobic mag-fura-2 experiments were carried out exactly as described previously (*16*, *25*) using a known concentration of apoprotein (20−50 μM) and mag-fura-2 (Molecular

Probes; also known as Furaptra, tetrapotassium salt) (16−18 μM) in buffer S. Following each *i*th addition of Zn(II), the spectra were collected from 240 to 900 nm, and the corrected absorbance at 366 and 325 nm was monitored and plotted as a function of total Zn(II) concentration. The metal concentration was checked by atomic absorption spectroscopy for each titration. The resulting binding curves at 366 and 325 nm were subjected to a simultaneous nonlinear least-squares fit to a simple competition model as described previously (*25*).

^{113}Cd NMR Spectroscopy. $^{113}CdCl_2$ (1.0 molar equiv) was added to the wild-type AztR sample which has been dialyzed against a deuterated HEPES buffer (5 mM Hepes-d_{18}, 0.35 M NaCl, 10% D_2O, pH 7.0) in the anaerobic glovebox. The resulting ^{113}Cd-substituted AztR was concentrated to ≈750 μM and then loaded anaerobically into a 10 mm (o.d.) NMR tube for NMR spectroscopy essentially as described previously (*18*). The ^{113}Cd NMR resonance frequency of AztR is reported relative to 0.1 M $Cd(ClO_4)_2$ acquired under the same solution conditions.

RESULTS

An analysis of the deduced amino acid sequence of the alr7622 ORF in the genome of *Anabaena* sp. strain PCC 7120 reveals that this gene encodes a putative CPx-ATPase, which we denote AztA. Hydropathy plot analysis predicts that AztA possesses eight transmembrane domains, as well as two soluble N-terminal metal-binding domains (MBDs) predicted to face the cytosol (data not shown). The amino acid sequence C-terminal to the N-terminal metal-binding domain in AztA exhibits a high percentage of sequence identity with known Zn(II)-transporting CPx-ATPases found in other cyanobacteria including Bxa1 (61%) (*23*) and ZiaA (59%) (*26*); this similarity is even higher in the eight putative transmembrane domains and the conserved motifs in all CPx-ATPases. Due to these similarities, these domains have been proposed to be important in metal ion transporting specificity (*27*). The high degree of sequence identity suggests that the function of AztA in *Anabaena* might be similar to other divalent transporting CPx-ATPases. However, AztA possesses two -DCxxC- metal-binding domains, each of which is followed by a His-rich motif (Figure 1C). A single DCxxC Atx1-like domain has been structurally characterized by NMR spectroscopy in ZntA, with Asp immediately preceding the first Cys thought to directly coordinate the metal ion and confer selectivity for Zn(II) over other cations (*12*). Up to this point, multiple CXXC metal-binding sites have been found only in the Cu(I)/Ag(I) translocating CPx-ATPases (*28*, *29*), while a His-rich domain has been found in a range of Zn(II)/Cd(II) CPx-ATPases (*13*, *30*). These characteristics make AztA distinct from other Cu(I) or Zn(II) transporting CPx-ATPases found thus far (Figure 1C) (*12*, *29*, *31*, *32*).

AztR shares a high degree of amino acid sequence similarity with other cyanobacterial Zn(II) repressors including the regulators of the expression of ZiaA and Bxa1, ZiaR (78%) and BxmR (73%), respectively, as well as SmtB (67%), the regulator of the *smt* operon in *Synechococcus*. However, AztR lacks the conserved ligands in the previously characterized zinc-sensing α5 site, in particular, that corresponding to His^{117} in SmtB and His^{97} in CzrA (*16*). In contrast, AztR conserves all three key ligands in the α3N

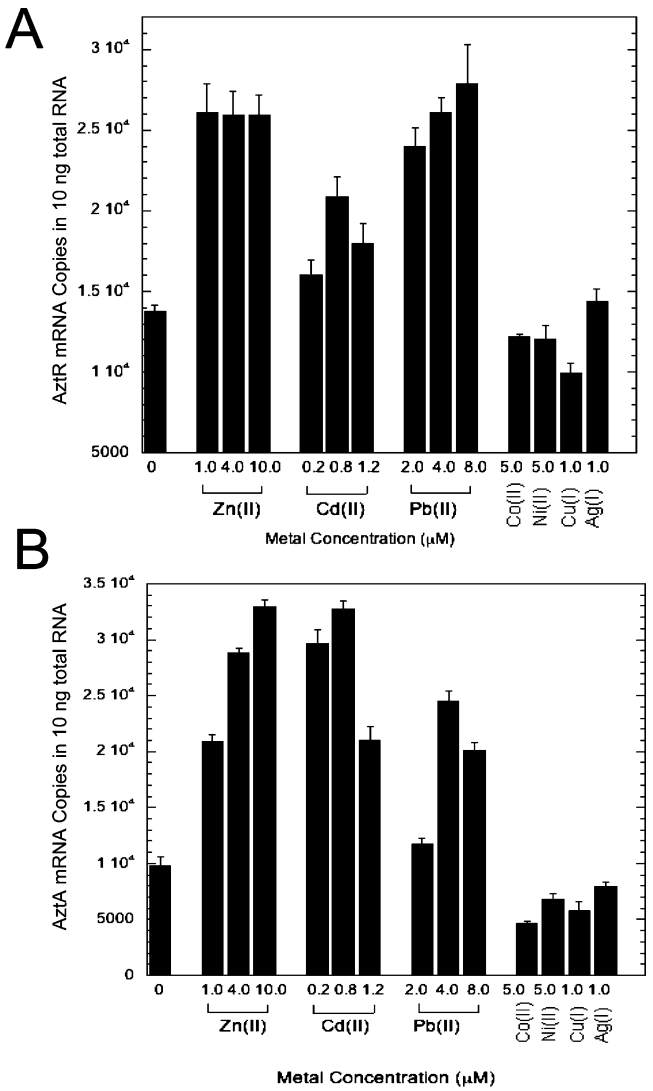

FIGURE 2: Quantification of the transcription of the genes encoding AztR (A) and AztA (B) in response to the indicated concentrations of metal ions in *Anabaena* PCC 7120 cultures. Pregrowth *Anabaena* PCC 7120 cells were treated with Zn(II), Pb(II), Cd(II), Co(II), Ni(II), Cu(II), and Ag(I) heavy metal ions for 2 h at the indicated concentration. Note that Cu was added as copper(II) sulfate to the media at the indicated concentration and is assumed to be Cu(I) in cells, and the background level of Zn(II) in the growth media is 0.7 μM. The absolute amount of mRNA was calculated from an external standard as described in Materials and Methods.

site, making it more similar to the Cd(II)/Pb(II)-regulated repressor, *L. monocytogenes* CadC (*17*).

Zn(II), Pb(II), and Cd(II) Upregulate the Expression of aztA/R in Anabaena PCC 7120. The in vivo *aztA/R* expression induced by divalent or monovalent metal ions was quantified using a real time RT-PCR assay. The expression of both AztR (Figure 2A) and AztA (Figure 2B) is induced ≈2−3-fold upon addition of micromolar amounts of Zn(II) to the growth culture [Zn(II) is 0.7 μM in the culture media]. This expression was stable over a wide range of Zn(II) concentrations (Figure 2A), even when the Zn(II) concentration was raised to 20 μM or more (data not shown). As anticipated, Cd(II) and Pb(II) are also inducers of AztR and AztA expression, with 0.2 μM Cd(II) capable of inducing *aztA* maximally (Figure 2). There is no significant induction of AztA and AztR expression by other divalent [Co(II), Ni(II)] or monovalent [Cu(I) and Ag(I)] metal ions over the

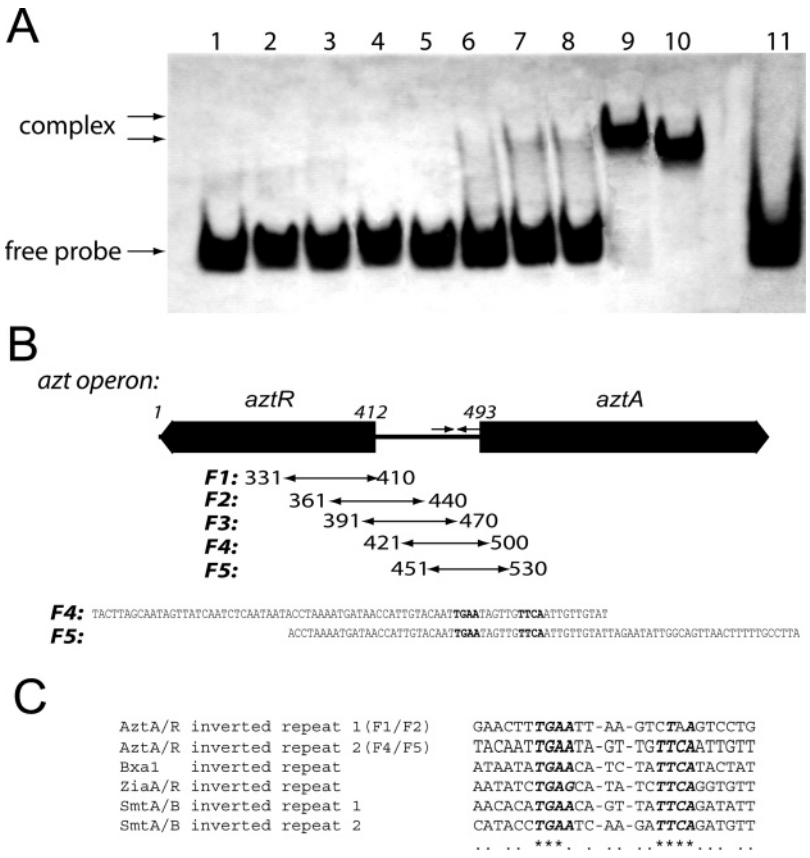

FIGURE 3: In vitro analysis of AztR binding ability to the operator/promoter region of the AztA/R operon. (A) Mapping the AztR/DNA binding fragment in the operator/promoter region of the *azt* operon. Lanes 1−5 and lanes 6−10 contained 1 nM free Dig-labeled DNA fragments F1 to F5 (sequences shown in panel B), respectively, in 15 μL reactions. Lanes 6−10 contained 0.67 μM purified wild-type apo-AztR. Lane 11 shows the same binding reaction as in lane 10 except for addition of a 100-fold excess of unlabeled F5. (B) Summary of the individual 80 bp Dig-labeled DNA fragments in the *aztR/A* operon. The sequences of fragments F4 and F5 are also given, with bold letters indicating the central part of a 12-2-12 inverted repeat in fragments F4 and F5. (C) The 12-2-12 inverted repeat sequences derived from the *aztA/R* F1/F2 fragment, *bxa1*, *zia*, and *smt* operator/promoter regions compared to the AztR binding site in *aztA/R* F4/F5.

same concentration range (Figure 2A). Since *aztR* and *aztA* expression is induced by the same spectrum of metals in a largely parallel fashion, we conclude that the *aztR/A* operon is a Zn(II)/Pb(II)/Cd(II)-specific responsive operon and AztR and AztA are cotranscribed.

Identification of AztR−DNA Binding Sites in the azt Operator/Promoter. Previous reports suggest that ArsR/SmtB regulators bind to the operator/promoter regions of the operon they regulate (*14*). We therefore hypothesized that this would also be the case for the *azt* operon. If this is indeed the case, the 182 bp region between the *aztR* and *aztA* genes should contain the regulatory DNA binding site(s) for AztR. Thus, gel mobility shift assays were employed to map the AztR DNA binding site using five overlapping 80 bp fragments derived from the putative *azt* promoter/operator region (Figure 3). As shown in Figure 3A, a gel mobility shift experiment identified two fragments, F4 and F5, that were capable of forming a single complex with slightly different mobilities with AztR; this suggested that a 50 bp overlapping region shared by these two fragments contains the primary sequence for the DNA−AztR interaction. Analysis of this overlapping fragment shows that it contained a 12-2-12 inverted repeat which is similar to those found in *smt*, *zia*, and *bxmR*/*bmtA* operons (*22*, *26*) (Figure 3C). In addition, given that the inverted repeat is offset in F4 vs F5 relative to the ends of the oligonucleotide and distinct mobilities result, AztR likely significantly bends the DNA. It is noticeable that F1 and F2 fragments also contain an overlapping imperfect inverted repeat (Figure 3C) that had been predicted previously to function as a protein−DNA binding site for AztR (*22*); however, these experiments reveal this is not the case, probably due to two bp substitutions in the downstream 5′-TGAA sequence (Figure 3C). The data reveal that there is only one AztR binding site in the *azt* operator/promoter, which agrees with the in vivo expression studies that suggest that AztA and AztR are cotranscribed.

Experiments designed to investigate the negative regulation of *azt* O/P binding effected by inducing metal ions were carried out by measuring a change in the fluorescence anisotropy of a 42 bp fluorescein-labeled *azt* O/P fragment upon AztR binding (bps 463−504; see Figure 3B) (*18*, *33*, *34*). These experiments reveal that a significant decrease in AztR−DNA binding affinity is achieved when AztR−Zn(II), AztR−Cd(II), or AztR−Pb(II) complexes are titrated into free DNA, as previously found for other ArsR/SmtB sensors (data not shown). These data are consistent with the finding that Zn(II), Cd(II), and Pb(II) are all negative regulators of *azt* operon binding by AztR.

The AztA/R Operon Functions as a Zn(II)/Pb(II) Resistance Determinant in E. coli. The results of the AztR−DNA binding experiments are in full agreement with the in vivo metal inducibility experiments. To confirm that AztR is the only regulator for the *aztA/R* operon in vivo, a sequence

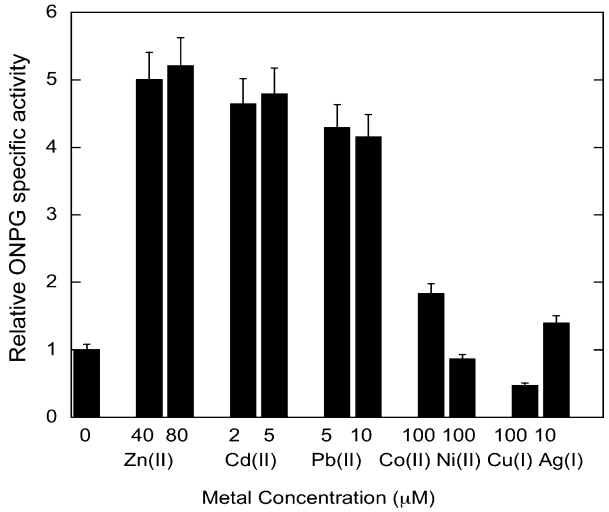

FIGURE 4: Induction of expression of the *aztR-lacZ* fusion by heavy metal ions in *E. coli*. The metals and concentrations are indicated [note that the indicated Pb(II) concentrations may be overestimated due to some precipitation of lead(II) phosphate salts in the media; note also the Cu was added as copper(I) sulfate]. The relative ONDG activity was generated by comparing the β-galactosidase activity before and after exposure to metal ions. The mean and standard deviation generated from at least three independent experiments are shown.

including the *aztR* gene and the operator/promoter region derived from the region immediately upstream of the *aztA* gene (see Figure 3) was cloned and fused to a promoterless *lacZ* gene, and *lacZ* expression in the presence and absence of metal ions was determined. Addition of Zn(II), Cd(II), and Pb(II) in growth media all result in significant transcriptional induction of *lac*Z gene expression, whereas other divalent or monovalent metal ions do not (Figure 4). These experiments confirm that the *aztRA* operator/promoter region and AztR itself are necessary and sufficient to confer Zn(II)/Pb(II)/Cd(II) responsiveness to a heterologous reporter gene and further suggest that the *aztRA* operon could be regulated in *E. coli* by the same panel of metal ions.

To test this, the entire *aztRA* operon was cloned into pET3a (pAztR/A) and transferred into Zn(II)/Cd(II)-hypersensitive *E. coli* strain GG48 (ΔzitB::Cm *zntA*::Km) (*21*). The expectation was that if AztA indeed functions as a Zn(II)/Pb(II)/Cd(II) efflux pump, significant metal resistance could be conferred on *E. coli* GG48. Under these conditions, 200 and 1000 μM total Zn(II) is sufficient to completely inhibit the growth of *E. coli* GG48 and wild-type *E. coli*, respectively (Figure 5A). Introduction of *aztR/A* into *E. coli* strain GG48 confers significant Zn(II) resistance, up to 800 μM Zn(II) (Figure 5A), an extent similar to that previously achieved with *Ralstonia metallidurans* ZntA under the same conditions [to 900 μM Zn(II)] (*35*). As expected, the addition of Pb(II) salts to pAztR/A-transformed GG48 also leads to significant Pb(II) resistance as well (Figure 5B).

In contrast to Zn(II) and Pb(II), the addition of Cd(II) to the media only confers marginal Cd(II) resistance in Zn(II)/Cd(II)-hypersensitive *E. coli* GG48, with complete growth inhibition occurring at 30 μM total Cd(II), relative to 10 μM in the vector-transformed control cells (Figure 5C). Note that wild-type *E. coli* W3100 can grow in Cd(II) concentrations as high as 700 μM, and transformation of GG48 with *R. metallidurans* CadA, a Cd(II)/Pb(II)-specific efflux pump, gives significantly greater Cd(II) resistance, up to 400 μM

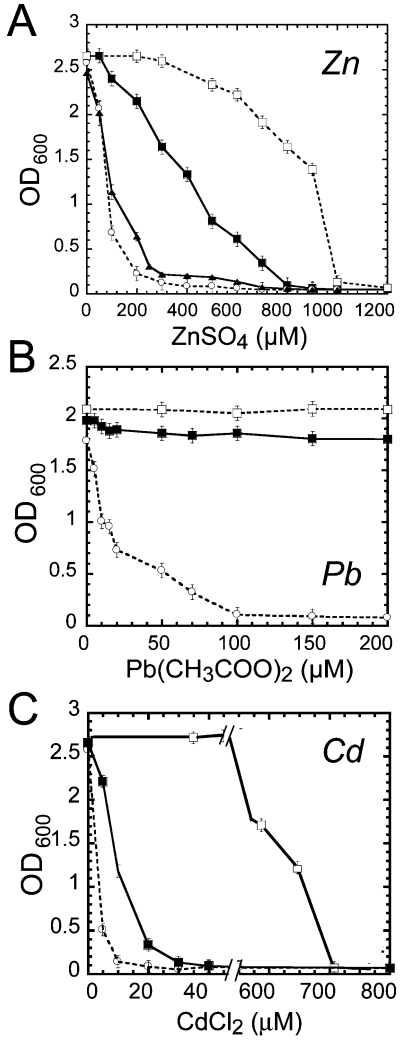

FIGURE 5: Introduction of the *azt* operon into Zn(II)/Cd(II)-hypersensitive *E. coli* GG48 confers significant resistance to Zn(II)/Pb(II) toxicity but limited resistance to Cd(II) salts. (A) Zn(II) resistance, (B) Pb(II) resistance, and (C) Cd(II) resistance, all at the indicated concentrations added [note that the Pb(II) concentrations indicated may be overestimated due to some precipitation of lead(II) phosphate salts in the growth media]. Representative data derived from measurements made in triplicate are shown for *E. coli* strain GG48 (ΔzntA ΔzitB) transformed with the pET3a vector (open circles), pETAztR/A (filled squares), and pETAztR/A_C74S AztR (filled triangles). Also shown are data obtained for the wild-type *E. coli* control (open squares).

(*35*). These results suggest that while Cd(II) is a significant inducer of the *azt* operon in both *Anabaena* sp. (Figure 2) and *E. coli* (Figure 4), Cd(II) may not be an efficient substrate for AztA, consistent with our previous findings that *Anabaena* has very low Cd(II) resistance (*23*). As expected from the metal inducibility profiles, there are no significant changes in Cu(I) and Ag(I) resistance in pAztR/A-transformed GG48 relative to vector-transformed control cells (data not shown). Taken together, these data show that the *aztRA* operon complements a Δ*zntA* knockout *E. coli* strain, consistent with the idea that, like ZntA in *E. coli*, the *azt* operon is involved in Zn(II) homeostasis in *Anabaena* sp. strain PCC 7120 by effluxing Zn(II) across the plasma membrane.

Metal-Binding Properties of Anabaena AztR. The in vivo induction experiments make the prediction that AztR would bind Zn(II), Cd(II), and Pb(II) directly in order to effect

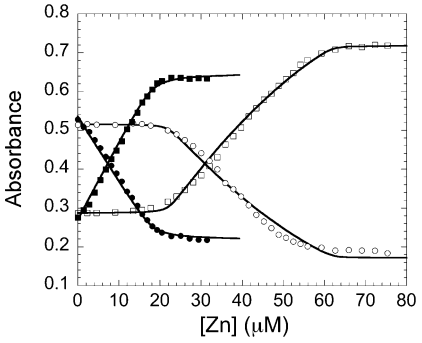

FIGURE 6: Anaerobic titration of Zn(II) into a mixture of mag-fura-2 and purified wild-type AztR (open symbols) or C74S AztR (filled symbols). Conditions: 10 mM HEPES, 0.4 M NaCl, pH 7.0, 40 μM monomer AztR or C74S AztR, and 16.7 μM mag-fura-2. Absorbance was at 366 nm (■, □) and 325 nm (●, ○). The solid line represents a simultaneous, nonlinear, least-squares fitting curve generated by Dynafit to a two-step sequential binding model. See text for details.

metalloregulation of the *azt* operon in vivo. The mode of Zn(II) binding by AztR is of particular interest because AztR does not harbor an α5-sensing site as mentioned (Figure 1B) (*34*); in contrast, sequence analysis suggests that AztR contains a CadC-like α3N site, with the residue corresponding to Cys11 in *S. aureus* pI258 CadC perhaps replaced by a His residue (His24 or His27); His24 in AztR is analogous to His18 in *Synechococcus* SmtB that has been postulated to donate a ligand to the α3N site in that protein (*16*, *25*). We note, however, that Cys11 is a weakly associated ligand to the Cd(II) ion in CadC and is excluded altogether from the trigonal-pyramidal Pb(II) complex (*17*, *36*) and is not required for metalloregulation in vitro (*17*) or in vivo (*37*).

(A) Zn(II) Binding to AztR. Zn(II) is spectroscopically silent, making it difficult to directly monitor Zn(II) binding to AztR. Therefore, the indicator dye mag-fura-2 was mixed with purified AztR and titrated with zinc in an anaerobic environment in order to determine stoichiometry and affinity of Zn(II) binding to AztR via a simple competition assay. Mag-fura-2 forms a 1:1 complex with Zn(II) with a K_{Zn} of 5.0×10^7 M^{-1}(*38*), which results in a significant shift in the absorption maximum from 366 to 325 nm. As shown in Figure 6 (open symbols), Zn(II) does indeed bind to AztR with the expected stoichiometry of 2 Zn(II) per AztR homodimer; however, their affinities are vastly different. The first equivalent of Zn(II) added binds to AztR with an affinity far greater than mag-fura-2 ($K_{Zn1} \gg 10^{10}$ M^{-1}) since there is no competition with the indicator dye up to 1 mol dimer equiv of Zn(II) (40 μM). After this point, the remaining Zn-(II) site on the AztR homodimer and mag-fura-2 have similar affinities, with complete saturation of mag-fura-2 occurring upon addition of ≈38 μM more Zn(II) [58 μM total Zn(II)], which equals the sum of the concentrations of remaining monomer sites (20 μM) and maga-fura-2 (18.0 μM). The solid curve through the data to a stepwise Zn(II)-binding model gives $K_{Zn2} = 2.3 \times 10^7$ M^{-1}. This is consistent with strong negative homotropic cooperativity, which has been also observed in other ArsR/SmtB regulators (*16*).

As expected, mutagenesis of the proposed α3N ligand Cys^{74} to serine reduces the affinity of both Zn(II)-binding sites on AztR to affinity far less that mag-fura-2 since C74S AztR is a poor competitor with mag-fura-2 for Zn((II) (Figure 6, filled symbols). The solid line returns $K_{Zn} \ll 5.0 \times 10^5$ M^{-1}, an upper limit under these conditions. Cys74 corresponds to the most important functional thiolate ligand in the Cd(II)/Pb(II)-sensing α3N site of CadCs (*17*). Consistent with these in vitro data, transformation of *E. coli* GG48 with the pAztR/A encoding mutant C74S AztR confers little Zn-(II) resistance above that of vector-transformed control cells (Figure 5A), revealing that this proposed α3N metal site in AztR is the sole functional metal-sensing site in vivo.

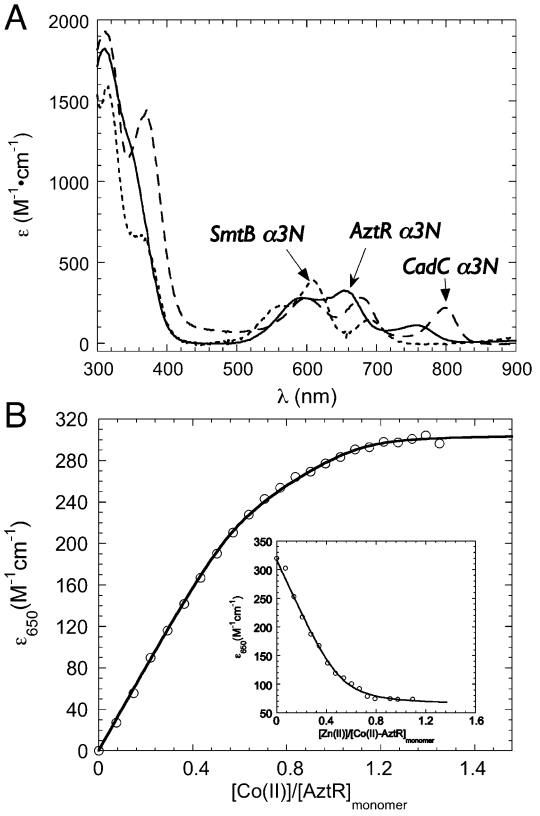

FIGURE 7: Optical absorption spectra of Co(II)-saturated AztR. (A) Co(II)-saturated AztR (solid line), Co(II)-saturated α3N site of *S. aureus* pI258 CadC (large dashed line) (*17*), and Co(II)-substituted α3N site of *Synechococcus* SmtB (dashed line) (*25*). (B) Co(II) binding isotherm generated from an anaerobic titration of Co(II) to wild-type AztR. The isotherm was plotted as ϵ_{650} vs [Co(II)]/total AztR monomer. The solid line represents a simultaneous, nonlinear, least-squares fitting curve generated by Dynafit with $K_{Co1} \geq 1.9 \times 10^7$ M^{-1} and $K_{Co2} = 4.5 \times 10^5$ M^{-1}. The value for K_{Co1} represents a lower limit given the high protein concentration used in this experiment. Inset: Zn(II) displacement titration of Co(II)-saturated AztR. Solution conditions: 10 mM HEPES, 0.4 M NaCl, pH 7.0, and 145 μM AztR. The isotherm was plotted as ϵ_{650} vs [Zn(II)]/total AztR monomer. The solid line has no physical meaning and is indicative of essentially stoichiometric displacement of Co(II) by added Zn(II).

(B) Co(II) Binding to AztR. Although in vivo studies show that Co(II) is not a strong inducer of the *aztAR* operon, the UV−visible absorption spectrum of the Co(II)-substituted AztR provides an excellent tool to determine the coordination sphere for Zn(II) in vitro (*39*). The UV−visible absorption spectral profile of Co(II)-substituted AztR (Figure 7A) reveals intense absorption in the near-ultraviolet (320 nm), which reports on contributions from the $S^- \rightarrow$ Co(II) LMCT transitions, and therefore is indicative of cysteine coordination (*39*); in the low-energy region, three well-resolved absorption bands positioned at 595, 655, and 755 nm are assignable to the $\gamma_3[^4A_2 \rightarrow {}^4T_1(P)]$ d−d electronic transition envelope characteristic of tetrahedral or distorted tetrahedral

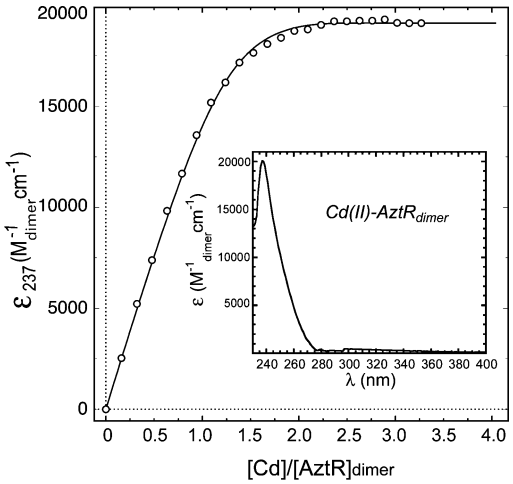

FIGURE 8: Anaerobic Cd(II)−AztR binding isotherm generated from optical spectra of AztR obtained on increasing concentrations of Cd(II). The plot was generated from ϵ_{237} vs total [Cd(II)]/total AztR homodimer ratio. The solid line represents a nonlinear, least-squares fitting curve generated by Dynafit with $K_{Cd1} \gg 2.0 \times 10^7$ M^{-1} and $K_{Cd2} = 1.4 \times 10^2$ M^{-1}. K_{Cd1} represents a lower limit given the high protein concentration used, while K_{Cd2} is likely meaningless and simply reflects the fact that the second Cd(II) ion binds weakly with an altered molar absorptivity. See text for details. Inset: Corrected [Cd(II)-bound AztR − apo-AztR] optical spectrum of Cd(II)-saturated wild-type AztR. Solution conditions: 10 mM HEPES, 0.4 M NaCl, pH 7.0, and 45.7 μM AztR.

metal coordination geometry (*40*). Although the spectra of Co(II)-saturated AztR is quite similar to two tetrahedral, tetrathiolate Co(II) coordination profiles published previously (*39*, *41*), the d−d ligand field envelope is moved to the blue relative to the highly distorted S_4 α3N of CadCs (*17*) and to the red when compared to the proposed S_2NO α3N complex in SmtB (Figure 7A) (*24*). In addition, the spectrum of the α3N metal complex of Co(II)-substituted ZiaR closely matches that of Co(II)-substituted AztR (*14*); ZiaR contains a His residue analogous to His27 in AztR. Since increasing cysteine thiolate coordination typically moves the d−d ligand field absorption envelope to lower energy, the absorption spectrum of Co(II)-AztR is most consistent with an S_3(N/O) first coordination shell, provided of course that the coordination geometries are largely similar in the comparison set (*42*). As expected from the Zn(II) binding studies above (Figure 6), Co(II)-substituted C74S AztR results in a loss of Co(II) binding to the α3N site (data not shown).

Co(II) binds to AztR with a molar ratio of 2 Co(II) to 1 AztR dimer (Figure 7B). However, as found for Zn(II) (Figure 6), the affinity of the first Co(II) is higher than the second with the continuous line through the data fit to a stepwise Co(II)-binding model, defined by $K_{Co1} > 1.9 \times 10^7$ M^{-1} and $K_{Co2} \approx 4.5 \times 10^5$ M^{-1}. As expected, Zn(II) titrated into a Co(II)-saturated AztR leads to a significant bleaching of the absorption spectrum of Co(II)-AztR (Figure 7B, inset); this reveals that Zn(II) and Co(II) occupy the same tetrahedral metal-binding site.

(C) Cd(II) Binding to AztR. UV−visible absorption spectra of wild-type apo-AztR titrated with Cd(II) (Figure 8, inset) show that formation of a Cd(II)−AztR complex results in a strong absorption at ≈237 nm. This intense absorption is attributable to S^- −Cd(II) ligand-to-metal charge transfer transitions with $\epsilon_{240} \approx 5500-6000$ $M^{-1}\cdot cm^{-1}$ per Cd−S bond (*17*, *43*). Shown in Figure 8 are corrected absorption spectra at 240 nm plotted as a function of Cd(II)/AztR$_{dimer}$ molar ratio. Consistent with Zn(II) and Co(II) titration results, AztR binds to Cd(II) with a stoichiometry of ≈2 Cd(II) per AztR homodimer; however, the molar absorptivities and affinities of the two bound Cd(II) ions are not equivalent. The solid curve through the experimental data, which reflects a nonlinear least-squares fit to a two-step sequential metal-binding model (as carried out above), clearly shows this. The molar absorptivity for the first bound Cd(II) is 17000 $M^{-1}\cdot cm^{-1}$ (Figure 8), consistent with ≈3 cysteine thiolate−Cd(II) coordination bonds in the α3N metal in AztR; in contrast, the second Cd(II) ion binds with strong negative cooperativity and a lower apparent molar absorptivity than the first Cd(II) ion. As expected, the molar absorptivity of the Cd(II) complex decreases to ≈5000 $M^{-1}\cdot cm^{-1}$ in C74S AztR (data not shown).

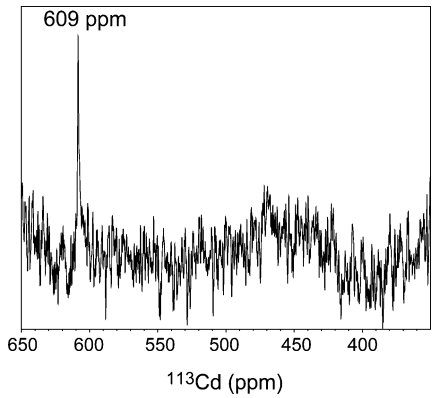

FIGURE 9: ^{113}Cd NMR spectroscopy of ^{113}Cd-substituted AztR wild-type protein. The chemical shift is reported relative to 0.1 M Cd-$(ClO_4)_2$. Conditions: 5 mM HEPES-d_{18}, 0.35 M NaCl, and 10% H_2O at pH 7.0 and 25 °C.

The ^{113}Cd(II) NMR spectrum of ^{113}Cd(II)-substituted AztR is compatible with the optical absorption spectra of Cd(II)- and Co(II)-substituted AztR (Figure 9). ^{113}Cd(II)-substituted AztR is characterized by a single ^{113}Cd(II) resonance positioned at 609 ppm, as anticipated for a tetrahedral S_3-(N/O) cadmium complex (*44*−*46*). It is interesting to note that this resonance is slightly upfield of the unusual, highly distorted S_4 *S. aureus* pI258 CadC complex ($\delta = 622$ ppm) (*18*) and downfield of the putative S_3O complex that characterizes C11G *S. aureus* pI258 CadC ($\delta = 590$ ppm) (*17*); the simplest interpretation of these data is that one of the two His in the N-terminal region of AztR (His24 or His27; Figure 1B) donates a ligand to the Cd(II) ion.

(D) Pb(II) Binding to AztR. The Pb(II) absorption spectra of Pb(II)-substituted AztR and C74S AztR are shown in Figure 10. Two intense $S^- \rightarrow$ Pb(II) LMCT or Pb(II) $\rightarrow S^-$ MLCT are observed. This spectrum is essentially identical to the Pb−S_3 and Pb−S_3 complexes of wild-type *S. aureus* pI258 CadC and HIV-CCHC zinc-binding domain (*17*, *47*), fully consistent with the trigonal-pyramidal complex formed by three thiolate ligands. Pb(II)−AztR binding isotherms appear to saturate at approximately 1 molar equiv of Pb(II) to 1 AztR homodimer, consistent with negative cooperativity of Pb(II) binding as well. As expected, substitution of Cys74 with Ser destroys the trigonal-pyramidal complex, with only apoprotein absorption observed in the ultraviolet region (Figure 10).

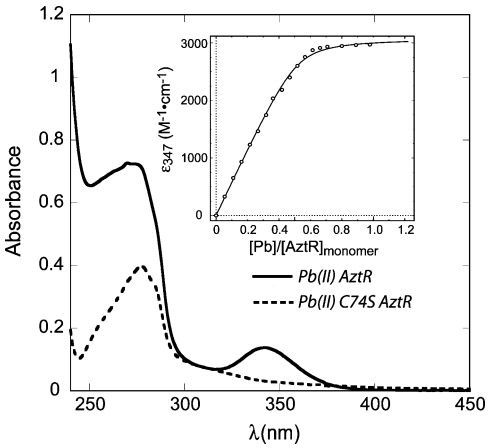

FIGURE 10: Optical absorption spectrum of Pb(II)-saturated AztR (solid line) compared to apo-AztR (dashed line). Inset: Pb(II) binding isotherm generated from Pb(II) optical spectra plotted as ϵ_{340} vs [Pb(II)]/total AztR monomer. The solid line represents a nonlinear least-squares fitting curve generated by Dynafit to a single-site binding model with $K_{Pb} = 1.4 \times 10^6$ M^{-1}. Solution conditions: 10 mM Bis-Tris, 0.4 M NaCl, pH 7.0, and 52.7 μM AztR.

DISCUSSION

In this paper, we report the identification and characterization of a novel Zn(II)/Pb(II)/Cd(II) efflux operon from *Anabaena* PCC 7120. This operon consists of a heavy-metal transporting CPx-ATPase designated AztA and an ArsR/SmtB family repressor designated AztR. The transmembrane domain of AztA shares high identity with other well-characterized Zn(II)-transporting CPx-ATPases (*13*, *26*). The metal-sensing repressor AztR shares high sequence similarity with SmtB-like zinc-sensing repressors found in other cyanobacteria, including *Synechococcus* SmtB (*48*), *Synechocystis* ZiaR (*26*), and *O. brevis* BxmR (*22*). However, AztR differs from these in one major way: it lacks the α5 zinc-specific binding site that is required for allosteric regulation of O/P binding by SmtB (*33*, *48*) and ZiaR (*26*). This makes AztR a closer structural and functional homologue of the well-characterized Cd(II)/Pb(II)-sensing repressor, CadC (Figure 1). On the other hand, *Synechocystis* ZiaR is capable of binding Zn(II) and Co(II) to both α3N and α5 sites (*14*), and introduction of nonliganding mutations in one or the other site appears to reduce metal-induced DNA dissociation (*26*).

Zn(II), Cd(II), and Pb(II) are significant transcriptional inducers of the *azt* operon, both in the native host *Anabaena* (Figure 2) and in *E. coli* (Figure 4). Interestingly, the induction of both AztR and AztA by Cd(II) and Pb(II) makes this operon different from other zinc-inducible operons including the *zia*, *smt*, and *czr* operons (*15*, *26*, *49*). The *azt* operon is also distinct from the *cad* operon of *S. aureus* pI258 since there is a significant induction by Zn(II) over a wide concentration range (*50*, *51*). Introducing a plasmid containing the entire *azt* operon to a Zn(II)/Cd(II)-hypersensitive *E. coli* GG48 functionally restores zinc tolerance to near wild-type *E. coli* 3100 levels but provides only moderate Cd(II) tolerance in this system. These in vivo data reveal that this Zn(II)/Pb(II)/Cd(II)-responsive operon functions as an effluxing transporter with a preference for zinc in the host *Anabaena*; however, Pb(II) and Cd(II) also induce the *azt* operon.

The AztR metal-sensing chelate adopts a distorted tetrahedral geometry (Figure 7), and ^{113}Cd NMR and optical absorption experiments are consistent with three cysteine thiolate donor atoms, proposed to be Cys21 from the N-terminal region and Cys72 and Cys74 (Figure 1B). Cys74 is clearly a critical metal ligand (Figures 5A and 10). The fourth ligand to the tetrahedral chelate is not yet known, but when compared with other α3N metal-sensing sites, the absorption spectrum of Co(II)-substituted AztR as well as the ^{113}Cd NMR chemical shift suggests that one of the two His in the N-terminal region (His24 or His27) conserved among ZiaR, SmtB, and BxmR provides the fourth ligand, creating an S_3N metal coordination complex. Attempts to measure one-bond coupling between ^{113}Cd and ^{15}N imidazole nitrogens in ^{15}N-labeled AztR (*52*) or three-bond coupling from ^{113}Cd to imidazole protons in unlabeled AztR (*53*) have thus far been unsuccessful under solution conditions where a subset of one-bond ^{113}Cd−^{15}N couplings are observable in the ^{113}Cd-substituted CzrA homodimer of similar molecular weight (A. Alphonse-Ignatius and D. Giedroc, unpublished observations). This suggests that if His24 or His27 is directly ligated to the Cd(II) ion, $^1J_{Cd-N}$ is smaller than in the α5-sensing site of CzrA; however, even in that case, only one of the three anticipated ^{113}Cd−^{15}N couplings is readily observed. In contrast to Zn(II), Cd(II), and Co(II), Pb(II) probably adopts a tris-thiolato coordination complex (Figure 10) (*17*).

What makes AztR an apparently better sensor of Zn(II) relative to CadCs? Although this is not known with certainty, an N-terminally derived His (His24 or His27) in place of a Cys in the first coordination shell to create a S_3N vs S_4 complex would likely make the relative affinities of Zn(II) and Cd(II) more similar than different (*54*); this might enable AztR to form more stable complexes with Zn(II) that compete well with the abundance of low molecular weight competitors in the cell. Alternatively, in the event of His−N^ϵ coordination, the His side chain can reach further than Cys, particularly in a highly distorted metal complex; this specific coordination bond might stabilize the chelate and help to drive allosteric coupling in this system. We are currently characterizing His substitution mutants of AztR, with both liganding (i.e., Cys) and nonliganding substitutions to test these ideas in vitro and in vivo. These studies will be interesting because Cys11 in CadC (which we propose is structurally analogous to His24 or His27 in AztR) is not required for Cd(II) sensing in vivo (*37*) or in vitro (*17*, *36*).

In all organisms, the detoxification of nonessential and toxic heavy metal ions usually shares the same or similar mechanisms of regulation, sequestration, and transport as essential metal ions (*55*). *Synechochoccus* SmtB, *S. aureus* CzrA, and *Mycobacterium tuberculosis* NmtR are three ArsR/SmtB family members that have evolved to sense biologically required borderline metals including Zn(II), Zn(II)/Co(II), and Ni(II)/Co(II), respectively, in their native hosts. The metal-sensing sites in each of these systems are a pair of symmetry-related interhelical, interprotomer metal chelates, designated α5, formed by a mixture of histidines and carboxylates and devoid of cysteine residues (*16*, *25*, *34*, *56*). This site likely resists distortion to accommodate larger metal ions including Cd(II) and Pb(II) and is not well-matched to coordinate these softer, more thiophilic metal ions. In fact, recent studies suggest that the substitution of

even one liganding residue with another non-native metal ligand reduces K_{Zn} by $\geq 10^4$-fold, thereby explaining the extraordinary evolutionary pressure to conserve all four α5 site metal ligands; thus it appears that this chelate may be thermodynamically and functionally optimized for this panel of biologically essential metal ions (M. Pennella and D. Giedroc, submitted for publication).

In contrast, in α3N-based ArsR/SmtB sensors that have been structurally characterized (*16*, *57*), the N-terminal domain in the apoprotein is unstructured. The implication is that this cysteine-rich α3N site near the periphery of the homodimer readily accommodates ions of different ionic radii and small changes in the coordination number and geometry, e.g., Cd(II) vs Pb(II). Such a metal-sensing site might be more amenable to evolutionary optimization, via ligand substitution, e.g., Cys for a His, in moving from CadC to AztR, that readily expands resistance to other toxic heavy metal ions. Recent structural data on Cu(I)-sensing vs Zn(II)-sensing MerR family metal sensors (CueR and ZntR) are consistent with this idea (*58*). In MerR proteins, a metal-binding loop that bridges a small region of the dimer interface has evolved to sense a wide range of thiophilic metals ions, from Cu(I) to Zn(II), Cd(II), and Pb(II), with specificity apparently largely achieved by changing the coordination number and ligand set in each case (*58*, *59*). A similar argument has been made for Cu(I)- vs Zn(II)-specific metal-binding domains found in copper(I) metallochaperones and metal efflux pumps, with Cu(I) binding with the bis- or tris-thiolate complex and Zn(II) forming complexes that recruit a "harder" carboxylate ligand into the complex (*12*) (see Figure 1C).

These studies with *Anabaena* AztR establish that the α3N metal site in ArsR/SmtB metal sensors is not confined to sensing only toxic metal ions Cd(II) and Pb(II) but is fully capable of sensing Zn(II) in non-native and native host backgrounds. This characteristic of AztR may have endowed *Anabaena* with having an evolutionary advantage to adapt to a broader range of heavy-metal environments by employing what is fundamentally a zinc-inducible efflux system to achieve detoxification of extremely toxic Cd(II) and Pb(II) ions that play no biological role. Our ongoing investigations of the function and regulation of a companion α5 site repressor, designated AzuR (alr0831; see Figure 1B), in *Anabaena* will provide us with additional insight into the biological contributions that these two distinct metal-binding sites play in what appears to be a simple zinc homeostasis system.

ACKNOWLEDGMENT

We acknowledge Mr. Rodrigo Mella for assistance with some of these experiments and Dr. Mario Pennella of the Biomolecular NMR Laboratory at Texas A&M University for help in acquiring the ^{113}Cd NMR spectrum. We also thank Christopher Rensing (University of Arizona) for the generous gift of *E. coli* strain GG48 and Dr. Mario Pennella for helpful comments on the manuscript.

REFERENCES

1. Finney, L. A., and O'Halloran, T. V. (2003) Transition metal speciation in the cell: insights from the chemistry of metal ion receptors, *Science 300*, 931−936.
2. McCall, K. A., Huang, C., and Fierke, C. A. (2000) Function and mechanism of zinc metalloenzymes, *J. Nutr. 130*, 1437S-1446S.
3. Auld, D. S. (2001) Zinc coordination sphere in biochemical zinc sites, *Biometals 14*, 271−313.
4. Patzer, S. I., and Hantke, K. (1998) The ZnuABC high-affinity zinc uptake system and its regulator Zur in *Escherichia coli*, *Mol. Microbiol 28*, 1199−1210.
5. Hantke, K. (2002) Members of the Fur protein family regulate iron and zinc transport in *E. coli* and characteristics of the Fur-regulated fhuF protein, *J. Mol. Microbiol. Biotechnol. 4*, 217−222.
6. Rensing, C., Ghosh, M., and Rosen, B. P. (1999) Families of soft-metal-ion-transporting ATPases, *J. Bacteriol. 181*, 5891−5897.
7. Rosen, B. P. (2002) Transport and detoxification systems for transition metals, heavy metals and metalloids in eukaryotic and prokaryotic microbes, *Comp. Biochem. Physiol., Part A: Mol. Integr. Physiol. 133*, 689−693.
8. Lutsenko, S., and Petris, M. J. (2003) Function and regulation of the mammalian copper-transporting ATPases: insights from biochemical and cell biological approaches, *J. Membr. Biol. 191*, 1−12.
9. Arguello, J. M. (2003) Identification of ion-selectivity determinants in heavy-metal transport P_{1B}-type ATPases, *J. Membr. Biol. 195*, 93−108.
10. Wernimont, A. K., Huffman, D. L., Lamb, A. L., O'Halloran, T. V., and Rosenzweig, A. C. (2000) Structural basis for copper transfer by the metallochaperone for the Menkes/Wilson disease proteins, *Nat. Struct. Biol. 7*, 766−771.
11. Ralle, M., Lutsenko, S., and Blackburn, N. J. (2004) Copper transfer to the N-terminal domain of the Wilson disease protein (ATP7B): X-ray absorption spectroscopy of reconstituted and chaperone-loaded metal binding domains and their interaction with exogenous ligands, *J. Inorg. Biochem. 98*, 765−774.
12. Banci, L., Bertini, I., Ciofi-Baffoni, S., Finney, L. A., Outten, C. E., and O'Halloran, T. V. (2002) A new zinc-protein coordination site in intracellular metal trafficking: solution structure of the Apo and Zn(II) forms of ZntA(46−118), *J. Mol. Biol. 323*, 883−897.
13. Tong, L., Nakashima, S., Shibasaka, M., Katsuhara, M., and Kasamo, K. (2002) A novel histidine-rich CPx-ATPase from the filamentous cyanobacterium *Oscillatoria brevis* related to multiple-heavy-metal cotolerance, *J. Bacteriol. 184*, 5027−5035.
14. Busenlehner, L. S., Pennella, M. A., and Giedroc, D. P. (2003) The SmtB/ArsR family of metalloregulatory transcriptional repressors: structural insights in prokaryotic metal resistance, *FEMS Microbiol. Rev. 27*, 131−144.
15. Kuroda, M., Hayashi, H., and Ohta, T. (1999) Chromosome-determined zinc-responsible operon *czr* in *Staphylococcus aureus* strain 912, *Microbiol. Immunol. 43*, 115−125.
16. Eicken, C., Pennella, M. A., Chen, X., Koshlap, K. M., VanZile, M. L., Sacchettini, J. C., and Giedroc, D. P. (2003) A metal-ligand-mediated intersubunit allosteric switch in related SmtB/ArsR zinc sensor proteins, *J. Mol. Biol. 333*, 683−695.
17. Busenlehner, L. S., Weng, T. C., Penner-Hahn, J. E., and Giedroc, D. P. (2002) Elucidation of primary (alpha(3)N) and vestigial (alpha(5)) heavy metal-binding sites in *Staphylococcus aureus* pI258 CadC: evolutionary implications for metal ion selectivity of ArsR/SmtB metal sensor proteins, *J. Mol. Biol. 319*, 685−701.
18. Busenlehner, L. S., Cosper, N. J., Scott, R. A., Rosen, B. P., Wong, M. D., and Giedroc, D. P. (2001) Spectroscopic properties of the metalloregulatory Cd(II) and Pb(II) sites of *S. aureus* pI258 CadC, *Biochemistry 40*, 4426−4436.
19. Wong, M. D., Lin, Y. F., and Rosen, B. P. (2002) The soft metal ion binding sites in the *Staphylococcus aureus* pI258 CadC Cd(II)/Pb(II)/Zn(II)-responsive repressor are formed between subunits of the homodimer, *J. Biol. Chem. 277*, 40930−40936.
20. Wu, X., Liu, D., Lee, M. H., and Golden, J. W. (2004) patS minigenes inhibit heterocyst development of *Anabaena* sp. strain PCC 7120, *J. Bacteriol. 186*, 6422−6429.
21. Grass, G., Fan, B., Rosen, B. P., Franke, S., Nies, D. H., and Rensing, C. (2001) ZitB (YbgR), a member of the cation diffusion facilitator family, is an additional zinc transporter in *Escherichia coli*, *J. Bacteriol. 183*, 4664−4667.
22. Liu, T., Nakashima, S., Hirose, K., Shibasaka, M., Katsuhara, M., Ezaki, B., Giedroc, D. P., and Kasamo, K. (2004) A novel cyanobacterial SmtB/ArsR family repressor regulates the expression of a CPx-ATPase and a metallothionein in response to both Cu(I)/Ag(I) and Zn(II)/Cd(II), *J. Biol. Chem. 279*, 17810−17818.

23. Liu, T., Nakashima, S., Hirose, K., Uemura, Y., Shibasaka, M., Katsuhara, M., and Kasamo, K. (2003) A metallothionein and CPx-ATPase handle heavy-metal tolerance in the filamentous cyanobacterium *Oscillatoria brevis*, *FEBS Lett. 542*, 159−163.
24. VanZile, M. L., Cosper, N. J., Scott, R. A., and Giedroc, D. P. (2000) The zinc metalloregulatory protein *Synechococcus* PCC7942 SmtB binds a single zinc ion per monomer with high affinity in a tetrahedral coordination geometry, *Biochemistry 39*, 11818−11829.
25. VanZile, M. L., Chen, X., and Giedroc, D. P. (2002) Structural characterization of distinct α3N and α5 metal sites in the cyanobacterial zinc sensor SmtB, *Biochemistry 41*, 9765−9775.
26. Thelwell, C., Robinson, N. J., and Turner-Cavet, J. S. (1998) An SmtB-like repressor from *Synechocystis* PCC 6803 regulates an zinc exporter, *Proc. Natl. Acad. Sci. U.S.A. 95*, 10728−10733.
27. Hou, Z. J., Narindrasorasak, S., Bhushan, B., Sarkar, B., and Mitra, B. (2001) Functional analysis of chimeric proteins of the Wilson Cu(I)-ATPase (ATP7B) and ZntA, a Pb(II)/Zn(II)/Cd(II)-ATPase from *Escherichia coli*, *J. Biol. Chem. 276*, 40858−40863.
28. Huster, D., and Lutsenko, S. (2003) The distinct roles of the N-terminal copper-binding sites in regulation of catalytic activity of the Wilson's disease protein, *J. Biol. Chem. 278*, 32212−32218.
29. Banci, L., Bertini, I., Ciofi-Baffoni, S., Gonnelli, L., and Su, X. C. (2003) Structural basis for the function of the N-terminal domain of the ATPase CopA from *Bacillus subtilis*, *J. Biol. Chem. 278*, 50506−50513.
30. Mills, R. F., Krijger, G. C., Baccarini, P. J., Hall, J. L., and Williams, L. E. (2003) Functional expression of AtHMA4, a P1B-type ATPase of the Zn/Co/Cd/Pb subclass, *Plant J. 35*, 164−176.
31. Arnesano, F., Banci, L., Bertini, I., Huffman, D. L., and O'Halloran, T. V. (2001) Solution structure of the Cu(I) and Apo forms of the yeast metallochaperone, Atx1, *Biochemistry 40*, 1528−1539.
32. Mitra, B., and Sharma, R. (2001) The cysteine-rich amino-terminal domain of ZntA, a Pb(II)/Zn(II)/Cd(II)-translocating ATPase from *Escherichia coli*, is not essential for its function, *Biochemistry 40*, 7694−7699.
33. VanZile, M. L., Chen, X., and Giedroc, D. P. (2002) Allosteric negative regulation of smt O/P binding of the zinc sensor, SmtB, by metal ions: a coupled equilibrium analysis, *Biochemistry 41*, 9776−9786.
34. Pennella, M. A., Shokes, J. E., Cosper, N. J., Scott, R. A., and Giedroc, D. P. (2003) Structural elements of metal selectivity in metal sensor proteins, *Proc. Natl. Acad. Sci. U.S.A. 100*, 3713−3718.
35. Legatzki, A., Grass, G., Anton, A., Rensing, C., and Nies, D. H. (2003) Interplay of the Czc system and two P-type ATPases in conferring metal resistance to *Ralstonia metallidurans*, *J. Bacteriol. 185*, 4354−4361.
36. Apuy, J. L., Busenlehner, L. S., Russell, D. H., and Giedroc, D. P. (2004) Ratiometric pulsed alkylation mass spectrometry as a probe of thiolate reactivity in different metalloderivatives of *Staphylococcus aureus* pI258 CadC, *Biochemistry 43*, 3824−3834.
37. Sun, Y., Wong, M. D., and Rosen, B. P. (2001) Role of cysteinyl residues in sensing Pb(II), Cd(II), and Zn(II) by the plasmid pI258 CadC repressor, *J. Biol. Chem. 276*, 14955−14960.
38. Walkup, G. K., and Imperiali, B. (1997) Fluorescent chemosensors for divalent zinc based on zinc finger domains. Enhanced oxidative stability, metal binding affinity, and structural and functional characterization, *J. Am. Chem. Soc. 119*, 3443−3450.
39. Pountney, D. L., and Vasak, M. (1992) Spectroscopic studies on metal distribution in Co(II)/Zn(II) mixed metal clusters in rabbit liver metallothionein 2, *Eur. J. Biochem. 209*, 335−341.
40. Taylor, J. S., Lau, C. Y., Applebury, M. L., and Coleman, J. E. (1973) *Escherichia coli* Co(II) alkaline phosphatase. Absorption, circular dichroism, and magnetic circular dichroism of the d−d electronic transitions, *J. Biol. Chem. 248*, 6216−6220.
41. Guo, J., and Giedroc, D. P. (1997) Zinc site redesign in T4 gene 32 protein: structure and stability of cobalt(II) complexes formed by wild-type and metal ligand substitution mutants, *Biochemistry 36*, 730−742.
42. Garmer, D. R., and Krauss, M. (1993) *Ab initio* quantum chemical study of the cobalt d-d spectroscopy of several substituted zinc enzymes, *J. Am. Chem. Soc. 115*, 10247−10257.
43. Pountney, D. L., Tiwari, R. P., and Egan, J. B. (1997) Metal- and DNA-binding properties and mutational analysis of the transcription activating factor, B, or coliphage 186: a prokaryotic C4 zinc-finger protein, *Protein Sci. 6*, 892−902.
44. Armitage, I. M., and Otvos, J. D. (1982) Principles and applications of ^{113}Cd NMR to biological systems, *Biol. Magn. Reson. 4*, 79−144.
45. Oz, G., Pountney, D. L., and Armitage, I. M. (1998) NMR spectroscopic studies of I = 1/2 metal ions in biological systems, *Biochem. Cell Biol. 76*, 223−243.
46. Giedroc, D. P., Johnson, B. A., Armitage, I. M., and Coleman, J. E. (1989) NMR spectroscopy of ^{113}Cd(II)-substituted gene 32 protein, *Biochemistry 28*, 2410−2418.
47. Payne, J. C., ter Horst, M. A., and Godwin, H. A. (1999) Lead fFingers: Pb^{2+} binding to structural zinc-binding domains determined directly by monitoring lead-thiolate charge-transfer bands, *J. Am. Chem. Soc. 121*, 6850−6855.
48. Turner, J. S., Glands, P. D., Samson, A. C. R., and Robinson, N. J. (1996) Zn^{2+}-sensing by the cyanobacterial metallothionein repressor SmtB: different motifs mediate metal-induced protein-DNA dissociation, *Nucleic Acids Res. 24*, 3714−3721.
49. Huckle, J. W., Morby, A. P., Turner, J. S., and Robinson, N. J. (1993) Isolation of a prokaryotic metallothionein locus and analysis of transcriptional control by trace metal ions, *Mol. Microbiol. 7*, 177−187.
50. Yoon, K. P., Misra, T. K., and Silver, S. (1991) Regulation of the cadA cadmium resistance determinant of *Staphylococcus aureus* plasmid pI258, *J. Bacteriol. 173*, 7643−7649.
51. Lebrun, M., Audurier, A., and Cossart, P. (1994) Plasmid-borne cadmium resistance genes in *Listeria monocytogenes* are similar to cadA and cadC of *Staphylococcus aureus* and are induced by cadmium, *J. Bacteriol. 176*, 3040−3048.
52. Legge, G. B., Martinez-Yamout, M. A., Hambly, D. M., Trinh, T., Lee, B. M., Dyson, H. J., and Wright, P. E. (2004) ZZ domain of CBP: an unusual zinc finger fold in a protein interaction module, *J. Mol. Biol. 343*, 1081−1093.
53. Kosa, J. L., Michelsen, J. W., Louis, H. A., Olsen, J. I., Davis, D. R., Berkerle, M. C., and Winge, D. R. (1994) Common metal ion coordination in LIM domain proteins, *Biochemistry 33*, 468−477.
54. Krizek, B. A., Merkle, D. L., and Berg, J. M. (1993) Ligand variation and metal ion binding specificity in zinc finger peptides, *Inorg. Chem. 32*, 937−940.
55. Hantke, K. (2001) Bacterial zinc transporters and regulators, *Biometals 14*, 239−249.
56. Cavet, J. S., Meng, W., Pennella, M. A., Appelhoff, R. J., Giedroc, D. P., and Robinson, N. J. (2002) A nickel-cobalt-sensing ArsR-SmtB family repressor. Contributions of cytosol and effector binding sites to metal selectivity, *J. Biol. Chem. 277*, 38441−38448.
57. Cook, W. J., Kar, S. R., Taylor, K. B., and Hall, L. M. (1998) Crystal structure of the cyanobacterial metallothionein repressor SmtB: A model for metalloregulatory proteins, *J. Mol. Biol. 275*, 337−346.
58. Changela, A., Chen, K., Xue, Y., Holschen, J., Outten, C. E., O'Halloran, T. V., and Mondragon, A. (2003) Molecular basis of metal-ion selectivity and zeptomolar sensitivity by CueR, *Science 301*, 1383−1387.
59. Chen, K., Yuldasheva, S., Penner-Hahn, J. E., and O'Halloran, T. V. (2003) An atypical linear Cu(I)-S2 center constitutes the high-affinity metal-sensing site in the CueR metalloregulatory protein, *J. Am. Chem. Soc. 125*, 12088−12089.

BI050450+